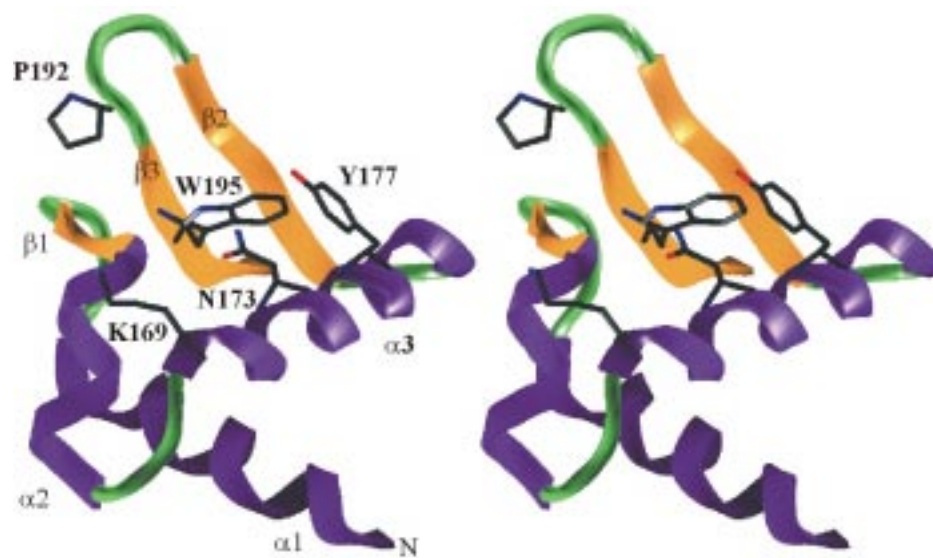


Structure and Function of the Z-DNA binding protein domain Z α



The solution structure of the Z α domain highlighting the most important Z-DNA contacting residues, as identified by scanning mutagenesis. The five alanine mutants, K169, N173, Y177, P192 and W195, showed the most dramatic reduction in affinity ($\Delta\Delta G$) to Z-DNA in quantitative binding assays using surface plasmon resonance (BIAcore) spectroscopy.

Aim of this work

Adenosine to inosine RNA editing in mammals changes the genetic information on the pre-mRNA level to produce proteins with modified function. To date, this has been observed for various subunits of AMPA- and kainate-sensitive glutamate receptors [1] and for serotonin-2C receptors [2] in the central nervous system. A candidate enzyme for catalyzing these RNA editing events, double-stranded RNA deaminase I (ADAR1), contains the N-terminal domain $Z\alpha$, which specifically binds to left-handed Z-DNA with high affinity *in vitro*, but whose function *in vivo* is unknown [3]. $Z\alpha$ is the first naturally occurring Z-DNA binding protein domain raising the question of how a protein can specifically recognize the left-handed conformation of DNA.

This Ph.D. thesis is aimed at exploring the functional and structural aspects of the interaction between $Z\alpha$ and Z-DNA. After the description of the experimental methods used for this work in chapter 1, the reader is introduced to protein/B-DNA interactions, to the biology of Z-DNA and to RNA editing in chapter 2. Chapter 3 centers on the stoichiometry and the binding constant of the $Z\alpha$ /Z-DNA interaction which was investigated by analytical ultracentrifugation, surface plasmon resonance and CD spectroscopy using a defined hairpin substrate, d(CG)₃T₄(CG)₃. By analytical ultracentrifugation and CD spectroscopy, it was found that two $Z\alpha$ domains bind to one hairpin in the Z-DNA conformation, while free $Z\alpha$ exists as a monomer [4]. The equilibrium dissociation constant (K_d) is 30 nM for one monomer, as measured by both analytical ultracentrifugation and surface plasmon resonance. Thus, the formation of a compact ternary ($Z\alpha$)₂/Z-DNA complex requires a binding site of no more than six basepairs.

In chapter 4, alanine scanning mutagenesis on $Z\alpha$ is used to identify residues that are pivotal for binding to Z-DNA. It was found that such residues cluster on one side of helix $\alpha 3$, making it likely that this area mediates Z-DNA contacts [5]. In addition, residues in $\alpha 1$, $\alpha 2$ and $\alpha 3$ were identified that probably form a hydrophobic core essential for protein stability. These data indicate that $Z\alpha$ shows structural similarity to ($\alpha+\beta$)-helix-turn-helix DNA binding proteins, such as HNF-3 γ and histone H5, in which $\alpha 3$ is used as a recognition helix. The mutational analysis is of particular importance because it paves the way for further functional studies, such as exploring the role of $Z\alpha$ *in vivo* by using loss-of-function mutants.

Chapter 5 describes the determination of the solution structure of free $Z\alpha$ whose interaction surface with the 6-basepair d(CG)₃T₄(CG)₃ hairpin is mapped by 2D ¹⁵N-HSQC NMR spectroscopy in chapter 6. These data allow a structural analysis of functional effects observed in the aforementioned mutational investigation. It was found that the interaction surface mapped in solution agrees well with the crystal structure of $Z\alpha$ complexed with Z-DNA [6]. The structure of $Z\alpha$ free in solution undergoes only minor conformational changes upon binding Z-DNA. Not only is the overall structure the same, but unexpectedly, most Z-DNA contacting residues are prepositioned in free $Z\alpha$ to fit Z-DNA [7].

The $Z\alpha$ domain shows close structural similarity to ($\alpha+\beta$) helix-turn-helix DNA binding proteins which exclusively bind to right-handed B-DNA [5]. In chapter 7, this study examines why $Z\alpha$ preferentially binds Z-DNA rather than B-DNA despite its high structural homology to ($\alpha+\beta$) helix-turn-helix B-DNA binding proteins. The comparison of $Z\alpha$ with the crystal structures of four homologous protein/B-DNA complexes suggests that binding of $Z\alpha$ to B-DNA is disfavored by steric hindrance.

ACKNOWLEDGMENTS

I wish to thank Prof. Alexander Rich and Prof. Günter Maaß for their supervision and kind support. I am particularly grateful to Dr. Alan Herbert for teaching me fundamental techniques of molecular biology with unparalleled enthusiasm, commitment and patience. He guided and supported this project from the very beginnings all the way through. I also want to thank Dr. Ky Lowenhaupt for critical discussion, helpful advice and thorough reviewing of several manuscripts. Furthermore, I wish to thank Mrs. Carolyn Beckman-Stitson for a warm welcome in the laboratory of Prof. Rich and advice in innumerable administrative respects. I express special thanks to Dr. Christopher Turner for his exceptional patience, humor and friendship while teaching me the principles and practice of NMR spectroscopy.

I am especially grateful to Prof. Hartmut Oschkinat for scientific and financial support and for giving me the opportunity to complete my Ph.D. thesis in his laboratory. Further thanks go to Dr. Peter Schmieder for practical and scientific assistance in many aspects of modern protein NMR spectroscopy. I am also grateful to Dr. Ronald Kühne for instant help with restrained molecular dynamics calculations and preparation of glossy figures. Furthermore, I wish to thank my other colleagues in the Oschkinat group for multifaceted assistance and helpful suggestions.

Most of all, I am indebted to my parents and my entire family who comforted me and provided moral support all along.

This Ph.D. thesis was supported by a fellowship from the Boehringer Ingelheim Fonds for biomedical research (Stuttgart, Germany).

List of Publications containing parts of this Ph.D. thesis

- 1) Schade, M.; Turner, C.J.; Kühne, R.; Schmieder, P.; Lowenhaupt, K.; Herbert, A.; Rich, A. and Oschkinat, H. „The solution structure of the Z α domain of the human RNA editing enzyme ADAR1 reveals a prepositioned binding surface for Z-DNA“ (1999) *Proc. Natl. Acad. Sci. USA*, **96**, 12465-12470.
- 2) Schade, M.; Behlke, J.; Lowenhaupt, K.; Herbert, A.; Rich, A. and Oschkinat, H. „A 6 bp Z-DNA hairpin binds two Z α domains from the human RNA editing enzyme ADAR1,, (1999) *FEBS Letters*, **458**, 27-31.
- 3) Schade, M.; Turner, C.J.; Lowenhaupt, K.; Rich, A. and Herbert, A. „Structure/function analysis of the Z-DNA binding domain Z α of dsRNA adenosine deaminase type I reveals similarity to the (α + β) family of helix-turn-helix proteins,, (1999) *EMBO J.*, **18**, 470-479.
- 4) Herbert, A.; Schade, M.; Lowenhaupt, K.; Alfken, J.; Schwartz, T.; Shlyakhtenko, L.S.; Lyubchenko, Y.L. and Rich, A. „The Z α domain from human ADAR1 binds to the Z-DNA conformer of many different sequences,, (1998) *Nucleic Acid Res.*, **26**, 3486-3493.

Contributions to Scientific Conferences

- 1) Markus Schade, „Structure/function analysis of the Z-DNA binding domain Z α of dsRNA adenosine deaminase type I reveals similarity to the (α + β) family of helix-turn-helix proteins“, 2nd Franco-German NMR meeting of the GDCh NMR Fachgruppe in Obernai, France, from 27.-30. September 1998 (Oral presentation)
- 2) Markus Schade, „Solution structure of the first Z-DNA binding protein domain Z α of the human RNA editing enzyme ADAR1“, 37th IUPAC Congress and 27th GDCh General Meeting“ in Berlin, Germany, from 14.-19. August, 1999 (Oral presentation)
- 3) Markus Schade, et al. „The solution structure of the Z α domain of the human RNA editing enzyme ADAR1 reveals a prepositioned binding surface for Z-DNA“, Meeting of the GDCh NMR-Fachgruppe in Würzburg, Germany from 29.9.-2.10.1999 (Poster presentation and Reception of a „R.R. Ernst Stipendium“)

TABLE OF CONTENTS

Aim of this work	i
Abbreviations	vii
Material and Methods:	vii
Biochemical terminology:	vii
NMR terminology:	viii
CHAPTER 1	1
Materials and Methods	1
Materials	1
Buffers and Solutions	1
Suppliers	1
Methods	3
Protein preparation	3
Analytical ultracentrifugation	4
Surface plasmon resonance	5
Circular dichroism spectroscopy	7
Bandshift and Southwestern assay	8
NMR spectroscopy	9
Interaction mapping	9
Structure calculation	9
CHAPTER 2	11
Introduction	11
Protein/DNA Interactions	11
Helix-turn-helix DNA binding proteins	11
(α + β)HTH DNA binding proteins	13
Zinc binding domains that bind to DNA	14
Leucine zipper DNA binding proteins	15
β -sheet DNA binding proteins	16
Immunoglobulin-like DNA binding domains	18
Combinatorial control of transcription	19
DNA bending and DNA kinking proteins	20
DNA bending through backbone contacts: The CAP domain	21
DNA bending by a β -stranded saddle: The TATA-box binding protein	21
DNA bending by an α -helical saddle: The SRY HMG domain	23
Summary	24
The left-handed Z-DNA conformation	26
The structure of Z-DNA	26
Z-DNA in the realm of biology	28
Z-DNA in prokaryotes	29
Z-DNA in eukaryotes	29
Potential roles of Z-DNA <i>in vivo</i>	30
RNA editing	31
Insertion/deletion RNA editing	31
Substitution RNA editing	32
Cytidine to Uridine RNA editing (and vice versa)	33
Adenosine to Inosine RNA editing	34
The RNA editing enzymes ADAR1/2	35
The substrate specificity of ADAR1/2	36

The domain structure of ADAR1/2	37
RNA editing and Z-DNA	39
CHAPTER 3	41
Affinity, stoichiometry and conformation of substrate DNA bound to Zα	41
Introduction	41
Results and Discussion	41
Two Z α domains bind to six d(CG) basepairs	42
Affinity of Z α to d(CG) ₃ T ₄ (CG) ₃ and polyd(CG)	44
Binding and dimerization of Z α -C125S mutant	45
Summary	46
CHAPTER 4	47
Scanning Mutagenesis of Zα	47
Mutagenesis and functional assays	47
The C-terminal β -sheet shows 2 distinct sides	48
Helix α 3 has characteristic properties of a recognition helix	49
Helix α 1 and α 2 have essential hydrophobic faces	51
Essential turn residues	52
CD analysis of Y177A and K181A	52
Discussion	53
Summary	55
CHAPTER 5	56
The solution structure of Zα	56
Introduction	56
Semi-automated resonance assignment	57
Sequential backbone assignment	58
Backbone assignment by homonuclear NMR experiments	58
Backbone assignment by ¹⁵ N-separated NMR experiments	59
Backbone assignment by triple resonance experiments	63
Side chain assignment	66
Assignment of aromatic side chains	68
Assignment of side chain ¹⁵ N resonances	68
Assignment of prolines and of residues preceding prolines	69
The secondary structure of Z α	69
Determination of dihedral phi angles	71
Summary	74
The tertiary structure of Z α	75
Introduction	75
Calculation of a template structure	76
Semi-automated NOE assignment	78
3D ¹⁵ N-HSQC-NOESY spectra	79
3D ¹³ C-HSQC-NOESY spectra	80
2D NOESY spectra in D ₂ O and H ₂ O	81
Calibration of distance restraints	83
Structure calculation	84
Distance geometry	85
Dynamic simulated annealing	85
Iterative structure refinement	86

Precision and quality of the final ensemble of Z α structures	87
The solution structure of Z α	89
Comparison of the Z α structure with mutants of the hydrophobic core	91
Summary	92
CHAPTER 6	94
The Interaction surface between Zα and Z-DNA	94
Mapping of the Z α /Z-DNA interaction surface in solution	94
Electrostatic potential surface of Z α	95
Comparison of the solution structure of free Z α with the crystal structure of Z α complexed with Z-DNA	96
Summary	99
CHAPTER 7	100
Biological implications of the Zα structure	100
Structural homologues of Z α	100
Steric hindrance disfavors B-DNA binding by Z α	101
Summary	102
CHAPTER 8	103
Outlook	103
CHAPTER 9	105
Appendix A	105
Principles of high-resolution NMR spectroscopy	105
The physical origin of NMR	105
The NMR signal	106
Relaxation	108
The chemical shift	109
Scalar (through bond) coupling: Coherence	110
Dipolar (through space) interaction: The NOE	112
Appendix B	115
Supplementary NMR data	115
Sequential assignment by triple resonance experiments	115
Chemical shift assignment list of Z α	116
HNH α coupling constants of Z α	121
Bibliography	124
Overview	133
Overall Summary of this Ph.D. thesis	133
Zusammenfassung der Doktorarbeit	134
Curriculum Vitae	135

ABBREVIATIONS

Material and Methods:

BSA	Bovine serum albumin
CD	Circular Dichroism
DSS	2,2-Dimethyl-2-silapentane-5-sulfonate, sodium salt
DTT	Dithiothreitol
EDTA	Ethylenediaminetetra-acetic acid
HEPES	(N-[2-Hydroxyethyl]piperazine-N'-[2-ethanesulphic acid])
Igepal	Non-ionic detergent
IPTG	Isopropyl- β -D-thio-galactopyranoside
LB	Luria Broth
MALDI-TOF	Matrix assisted laser desorption ionization-time of flight (mass spectroscopy)
OD	Optical density
PAGE	Polyacrylamide electrophoresis
PMSF	Phenyl-methanesulfon-fluoride
PBS	Phosphate buffered saline
rpm	Revolutions per minute
RU	Response Units (for BIAcore machine)
SDS	Sodium dodecyl sulfat
SE	Standard error
SPR	Surface plasmon resonance
Tris	Tris(-hydroxymethyl)-aminomethane
UV	Ultra violet

Biochemical terminology:

ADAR	Adenosine deaminase dsRNA-specific (formerly: dsRNA deaminase)
AMPA	α -Amino-3-hydroxy-5-methyl-4-isoxalepropionate
APOBEC1	<i>apoB</i> mRNA editing cytidine deaminase 1
bp	basepair
cAMP	cyclo-Adenosine-mono-phosphate
CAP	Catabolite activator protein
DNA	Deoxyribonucleic acid
DtxR	Diphtheria toxin repressor
ds	double-stranded
GST	Gluthathione-S-transferase
HNF-3 γ	Hepatocyte nuclear factor 3 γ
HMG	High mobility group
HTH	Helix-turn-helix
K _d	Equilibrium dissociation constant
LEF-1	Lymphoid enhancer-binding factor 1
NFAT	Nuclear factor of activated T-cells

RED2	dsRNA editase 2
rmsd	root mean standard deviation
RNA	Ribonucleic acid
SRY	sex-determining region Y
TBP	TATA box binding protein

NMR terminology:

COSY	Correlation spectroscopy
FID	Free induction decay
FT	Fourier transformation
HSQC	Heteronuclear single quantum correlation
INEPT	Insensitive nucleus enhancement by polarization transfer
NMR	Nuclear Magnetic Resonance
NOE	Nuclear Overhauser effect
NOESY	Nuclear Overhauser enhancement (effect) spectroscopy
ppm	Parts per million
rf	Radio frequency (pulse)
T ₁	Longitudinal (= spin-lattice) relaxation time
T ₂	Transverse (= spin-spin) relaxation time
TOCSY	Total correlation spectroscopy

Chapter 1

MATERIALS AND METHODS

Materials

If not otherwise specified all organic and inorganic chemicals were purchased in the highest available quality from Sigma (St. Louis, MO, USA) or Aldrich (Milwaukee, WI, USA). For enzymes and related biochemicals, the common vendor was New England Biolabs (Beverly, MA, USA).

Buffers and Solutions**Phosphate buffered saline (PBS buffer, pH 7.3):**

140 mM NaCl, 2.7 mM KCl, 10 mM Na₂HPO₄, 1.8 mM KH₂PO₄

M9 Minimal Medium (1x):

Na ₂ HPO ₄ *7H ₂ O	48 mM	12.8 g	per liter H ₂ O
KH ₂ PO ₄	22 mM	3.0 g	per liter H ₂ O
NaCl	9 mM	0.5 g	per liter H ₂ O
NH ₄ Cl	19 mM	1.0 g	per liter H ₂ O
MgSO ₄	2 mM	add as sterile solution separately	
CaCl ₂	0.1 mM	add as sterile solution separately	
Glucose	0.4 %	add as sterile 40 % solution separately	

Suppliers

BioRad, BioRad, Melville, NY
 Bruker GmbH, Rheinstetten, Germany
 CalBiochem, La Jolla, CA, USA
 Clontech, Palo Alto, CA, USA
 Cromassie Brilliant Blue dye (Instaview universal, BDH laboratory, Poole, GB)
 Dupont, Wilmington, DE, USA
 GibcoBRL, Gaithersburg, MD, USA
 Isotec Inc., Miamisburg, OH, USA
 Kirkegaard & Perry labs, Gaithersburg, USA
 Martek Biosciences Corp., Columbia, MD, USA
 Millipore Corp., Bedford, MA, USA

MSI, Molecular Simulations Inc., San Diego, CA, USA

New England Biolabs, Beverly, MA, USA

Novagen, Madison, WI, USA

Pharmacia, Piscataway, NJ, USA

Pierce, Rockford, IL, USA

Sigma, St.Louis, MO, USA

SLM Instruments Inc., Urbana, IL, USA

Sorvall Instruments, Wilmington, DE, USA

Stratagene, La Jolla, CA, USA

Tripos Inc., St.Louis, MO, USA

Methods

Protein preparation

Site-specific Z α mutants were constructed by PCR-based site-directed mutagenesis (QuikChange site-directed mutagenesis kit, Stratagene) and checked by DNA sequencing. Mutant and wild-type Z α proteins containing residues 120-197 of human ADAR1 (GenBank accession no. U10439), were expressed as Glutathione-S-Transferase(GST)-fusion proteins (GST is N-terminal) in pGEX-5x1 vectors (Pharmacia) in *E.coli* strain DH-5 α (GibcoBRL). The cells were grown at 37° C in 450 mL cultures of LB-medium containing 2 % glucose and 50 μ g/mL ampicillin. At an optical density (OD) of 1.0 at 600 nm, the cells were induced with 1 mL 100 mM IPTG and grown for another hour. The cells were harvested by centrifugation at 6000 rpm for 30 min at 4° C (rotor SS34, Sorvall Instruments), resuspended in 10 mL phosphate buffered saline (PBS) containing 0.1 mM protease inhibitor PMSF, and lysed by French pressing (SLM Instruments) at a pressure of 950 psi. The GST-fusion protein was purified by affinity chromatography using glutathione-agarose (Sigma). The soluble fraction of the lysed cells was loaded on a 300 mg glutathione-agarose column (10 mL disposable column, Pierce) and eluted with 10 mL PBS containing 10 mM glutathione. Proteins were checked by SDS-PAGE on 15 % gels and probed for binding to Z-DNA by bandshift and Southwestern assays.

For the preparation of Z α peptides, GST-fusion proteins were digested on-column with factor Xa protease (New England Biolabs) in 20 mM HEPES (pH 8), 100 mM NaCl, 2 mM CaCl₂, 0.05% n-Octyl-glucopyranoside at 22° C over night. The Z α peptides were washed off the column with the same buffer at pH 7.4 containing 1 mM DTT. These Z α peptides were checked by SDS-PAGE on 18 % gels and tested for binding to Z-DNA by bandshift assays.

Key Z α mutants were further investigated by surface plasmon resonance and CD spectroscopy. These mutants and a wild-type control comprising residues 122-197 of ADAR1, were expressed in pET-28a vectors in *E.coli* strain Novablue (Novagene). The pET-28a encoded construct differs from the pGEX-5x1-derived peptides in having a stop codon after I197, deleting 12 residues encoded by the pGEX-5x1 polylinker. In addition, the pET-28a construct, which is called the short Z α construct, contains five vector-encoded residues (GSHMG) in the N-terminus compared with three residue (GIP) in the pGEX-5x1 vector construct. Proteins were purified in two steps. First, the *E.coli* lysate was passed over a (His)₆-tag affinity column (TALON Metal Affinity Resin, Clontech) in 20 mM Tris/HCl (pH 8), 150 mM NaCl, using a 0 - 300 mM imidazole gradient for elution. The (His)₆-tag was removed by thrombin digestion (CalBiochem) in the same buffer. For the second purification step, protein was loaded on a cation exchange chromatography column (Mono S 5/S, Pharmacia) in 50 mM HEPES (pH 7.4), 25 mM NaCl, 1 mM EDTA, 1 mM DTT, 0.125 mM PMSF and eluted with a 25 - 1000 mM NaCl gradient, yielding homogeneous protein of wild-type molecular weight, as indicated by SDS-PAGE analysis and by MALDI-TOF mass spectroscopy.

For NMR, analytical ultracentrifugation and surface plasmon resonance measurements on wild-type and C125S mutant Z α , a different pET-28a construct was used which is referred

to as the long Z α construct in the following text. It comprises residues 119-200 of human ADAR1 and three additional vector-encoded residues: a glycine and a serine residue at the N-terminus and an aspartic acid at the C-terminus. The protein preparation was identical to that used for the short pET-28a construct.

For isotope labeling, the pET-28a vector (residues 119-200) was transformed into *E.coli* strain HM174(DE3) (Novagen), and the bacteria were grown in M9 minimal medium containing 1 g/L $^{15}\text{NH}_4\text{Cl}$ (Isotec Inc.) and 1.5 g/L ^{13}C -glucose (Martek Biosciences). The protein purification was unchanged.

Analytical ultracentrifugation

Analytical ultracentrifugation is a widely applied technique to study the molecular weight and hydrodynamic properties of biological macromolecules in solution. In sedimentation velocity experiments, the centrifugal force moves solute macromolecules at a certain rate to the bottom of the centrifuge cell. The rate per unit centrifugal field, s , is proportional to the molecular weight and inversely proportional to the frictional coefficient, which contains information about the shape of the macromolecule [8]. In sedimentation equilibrium experiments, the centrifugal force on a macro-molecule is balanced by diffusion leading to an equilibrium distribution of the macromolecule, from which its molecular weight can be determined. If two different macromolecules that bind to each other can be discriminated in the ultracentrifuge, for instance by their UV absorbance (fig. 1), the binding constant can be determined from the analysis of their equilibrium distribution. Thus, analytical ultracentrifugation is a powerful technique to investigate binding equilibria of unknown

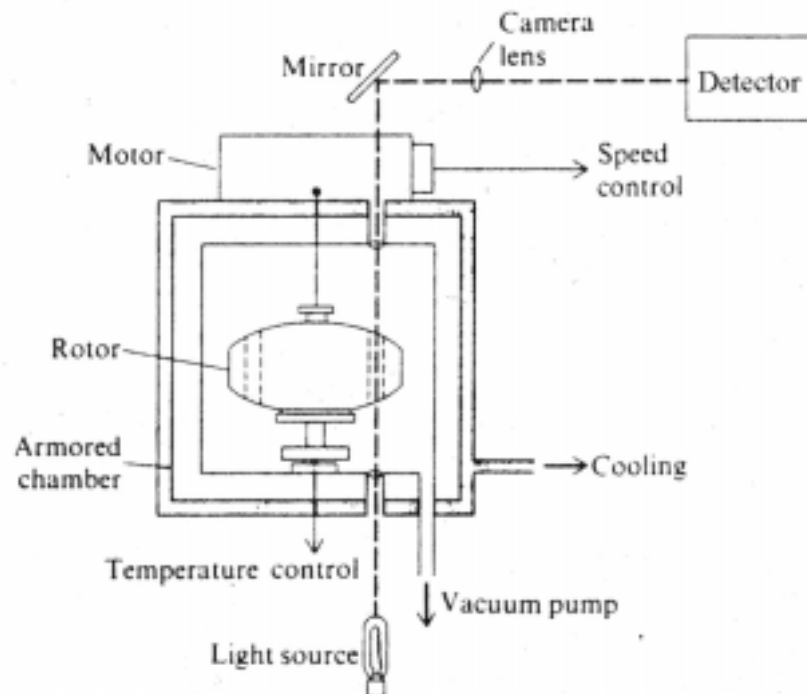


fig. 1 An analytical ultracentrifuge. Samples spinning in transparent sector cells within the rotor are monitored online either by UV/VIS spectroscopy or interference spectroscopy (Light source, Detector system).

stoichiometry.

Analytical ultracentrifugation experiments were performed on a Beckman XL-A ultracentrifuge in 10 mM Na-phosphate buffer (pH=5.5), 137 mM NaCl. Sedimentation velocity experiments were performed in standard double sector cells at 20°C. Equilibrium experiments were performed at 10°C in six channel cells making use of the overspeed technique. Here, the samples were centrifuged 2 h at 24000 rpm (overspeed step), and were subsequently spun at an equilibrium speed of 20000 rpm for 30 – 32 h (equilibrium step). The radial concentration profile of the d(CG)₃T₄(CG)₃ hairpin and the Z α protein was measured by UV absorption at six equidistant wavelengths ranging from 255 – 285 nm. The approximate extinction coefficients were calculated from the sequences as described for the DNA [9] and the protein [10].

Data collection and analysis of the four component system, free hairpin, free Z α , complex Z α /hairpin and (Z α)₂/hairpin, required a two-step approach. First, the molecular weights of both the hairpin and the Z α protein alone were determined by fitting the radial concentration profiles in sedimentation velocity and equilibrium experiments as described [11] [12]. These data were used to reduce the number of variables in the equation describing the four component system. Second, the concentration profiles of the complex were measured in a titration series with increasing protein concentrations. Protein concentrations from 0.7 to 6.0 μ M were tested in the presence of 1.8 μ M hairpin. The experimental concentration profiles were fitted to the sum of an exponential function for each of the four species as described [11] [13]. This global fitting was performed for the various Z α /hairpin ratios of the titration yielding the equilibrium dissociation constant, K_d. The resulting ratios of bound Z α /hairpin yielded a binding curve (Fig. 2B), from which the binding stoichiometry was obtained. Since the partial concentrations for the Z α /hairpin and (Z α)₂/hairpin complex in the titration are well described by a statistical binding model assuming identical binding sites, a single mean K_d for both binding steps was determined. The robustness and accuracy of this fitting procedure has been shown for other binding equilibria [11] [13].

In order to maintain cysteine 125 of wild-type Z α in the reduced form, the ultracentrifugation runs with wild-type protein were performed under strongly reducing conditions (100 mM β -mercaptoethanol). This was not necessary for the Z α -C125S mutant.

Surface plasmon resonance

Surface plasmon resonance (SPR) spectroscopy is a time-efficient technique to measure both binding constants and binding kinetics of interactions involving biological macromolecules. In a SPR spectrometer, which is more commonly known as a BIAcore instrument, a light beam is directed under a fixed angle onto a very thin golden chip (fig. 2). The intensity of the refracted light, which hits on the detector, is dependent on the refractive index of the solution on the opposite side of the golden chip. On this side, the molecule under investigation is immobilized. If a ligand binds to that molecule the refractive index changes leading to a signal on the detector that is proportional to the total mass bound. By passing a constant flow of buffer with and without ligand over the surface of that chip, binding and dissociation of this ligand can be monitored as a function of time. These data allow the calculation of binding rates and binding constants.

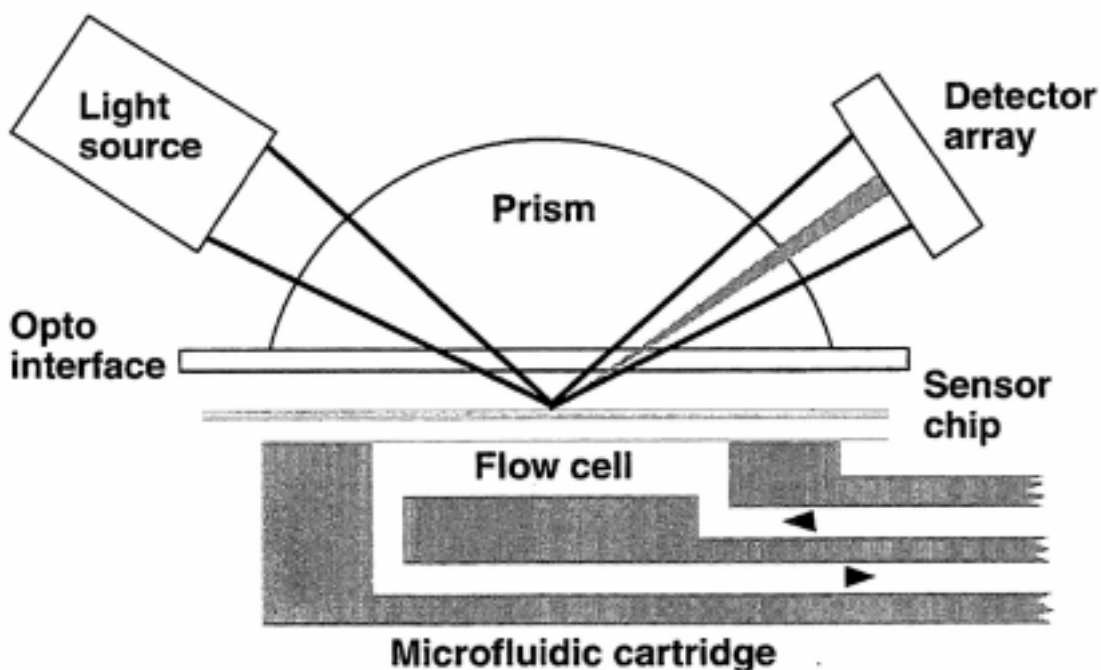


fig. 2 **Application of surface plasmon resonance (SPR) for measuring binding kinetics in solution.** A ligand (in this case DNA), which has been immobilized on the sensor chip, projects into the aqueous solution of the flow cell. An analyte (in this case wild-type and mutant $Z\alpha$ protein) is passed over the chip surface at a constant flow rate allowing the analyte to bind to the immobilized ligand. Bound analyte changes the refractive index leading to signal on the light detector that is proportional to the mass of analyte bound.

The total mass of ligand binding to or dissociating from the immobilized molecule is measured in arbitrary units, designated Response Units (RU). The detection of the change in total mass bound brings about the advantage that labeling of the ligand and knowledge of its physical properties is not required for detection. However, the detection of mass necessitates that the molecular weight of ligands is greater than approximately 1 kD, thereby limiting the range of ligands that can be studied by SPR. In most cases, the ligand can be washed off the chip allowing multiple measurements in a row on the same chip surface. Thus various ligands, such as different mutants of the $Z\alpha$ protein, can be tested under identical conditions in an automated binding assay.

The binding constants of mutant and wild-type $Z\alpha$ were measured on a BIAcore 2000 instrument. 270 Response units (RU) of polyd(CG) stabilized in the Z-DNA conformation by chemical bromination was immobilized on the chip surface through a biotin linkage. Protein solutions at different concentrations were passed over the chip surface with a flow rate of 20 $\mu\text{L}/\text{min}$ in phosphate buffer (pH 7.4), 137 mM NaCl, 1mM EDTA and 1 mM DTT. The change in surface plasmon resonance was determined at a data collection rate of 1 Hz. The baseline obtained by traversing the protein solution in line over a second chip surface lacking immobilized DNA was subtracted from each experimental curve. The $Z\alpha$ protein does not bind

to a random sequence B-DNA polymer of the same size and immobilized at the same density as the Z-DNA probe [3].

Binding curves were analyzed both by least square fitting to Langmuir isotherms and by time-resolved global analysis (BIAevaluation software 3.0 with mass transport correction) to cross-validate the equilibrium dissociation constant (K_d). The apparent on-rates for Z α and Z α -C125S were faster than $10^6 \text{ M}^{-1}\text{s}^{-1}$ and are affected by mass-transport artifacts [14]. Therefore, for calculation of the K_d , steady-state fitting to Langmuir isotherms was considered to be more robust. The protein concentrations used to measure the steady-state response covered an approximately 10-fold concentration range around the K_d of wild-type or mutant protein. Measurement at high flow rates of 50 and 100 $\mu\text{L}/\text{min}$ did not improve the quality of the data significantly. Fast binding rates are common for protein/DNA interactions. Furthermore, it is possible that Z α binding is considerably accelerated through 1D diffusion on the polyd(CG) string as compared with a 3D search for free binding sites.

For the K_d measurements of wild-type and C125S mutant protein, the long Z α construct was used which was also utilized for analytical ultracentrifugation and NMR spectroscopy. In contrast, the short Z α construct (residues 122-197) was used for the investigation of Z α mutants from $\alpha 3$ and the C-terminal β -sheet by surface plasmon resonance. This short Z α protein showed a K_d of $70 \text{ nM} \pm 30\%$ which is greater by a factor of 2.3 than the K_d (30 nM) obtained for the long Z α construct (residues 119 – 200). The NMR structure of Z α shows long-range NOEs for residue A198 suggesting that A198 is an integral part of the Z α core fold. Therefore, the C-terminal β -sheet of the short Z α construct, which lacks A198, may be less stable than that of the long Z α construct. This may explain the two-fold reduction in binding affinity because four residues in the C-terminal β -sheet mediate Z-DNA contacts in the crystal structure of the (Z α)₂/Z-DNA complex [6].

Circular dichroism spectroscopy

The circular dichroism (CD) titration of 10 μM d(CG)₃T₄(CG)₃ hairpin with increasing amounts of Z α protein (fig. 20) was recorded in 10 mM Na-phosphate buffer (pH 5), 75 mM NaF, 0.1 mM NaN₃ at 21° C on a Jasco J-720 CD spectrometer using a cuvette with a 10 mm pathlength. After 15 min of thermal equilibration, data were acquired at 0.1 nm resolution with a scan speed of 50 nm/min. The mean of six data accumulations was smoothed with a third order polynomial function. The characteristic CD spectrum of d(CG) oligomers in the Z-conformation at high ionic strength (4 M NaCl) is shown elsewhere [15].

The CD spectra of mutant and wild-type Z α alone (data not shown) were recorded at 5 μM in 10 mM Na-phosphate (pH 7.2), 137 mM NaCl and H₂O at 25 °C on an Aviv 60DS CD spectrometer using a cuvette with a 5 mm pathlength.

The CD spectra showing the B- to Z-DNA transition induced by the mutants Y177A and K181A, and by Z α wild-type (fig. 26), were acquired at 30° C in 50 mM Tris/HCl (pH 7.4), 25 mM NaCl and 0.1 mM EDTA on the Aviv CD spectrometer using the 5 mm cuvette. For CD titrations, polyd(CG) (50 μM bp concentration) was titrated with mutant and wild-type Z α in 6:1, 3:1 and 1:1 (mole bp) : (mole Z α) ratios. The stoichiometric ratio is 3:1 (mole bp) : (mole Z α) reflecting that two Z α domains bind to six d(CG) basepairs.

Bandshift and Southwestern assay

Bandshift assays, which are also called gelshift and electromobility shift (EMSA) assays, are widely used to measure the binding of a protein to nucleic acids or to other proteins. For bandshift assays the binding partners are pre-incubated for a few minutes and are loaded on a native polyacrylamide gel, in which the bound and free species are separated by electrophoresis. For the study of protein/DNA interactions, the DNA is commonly radioactively labeled with ^{32}P allowing both qualitative detection by autoradiography films and quantitative detection by phosphor-imaging instruments.

The study of protein/Z-DNA interactions by bandshift assays requires a special Z-DNA probe that maintains the Z-DNA conformation under near physiological conditions. This has been achieved by incorporating 5-bromo-desoxycytidine triphosphate and (α - ^{32}P)-labeled dGTP into a $\text{d}(\text{CG})_n$ polymer using the Klenow fragment of *E. coli* [16]. The bromination ensures that the DNA probe adopts the Z-DNA conformation at Mg^{2+} concentrations of 10 mM. This $(5\text{-Br-dCdG})_{33}$ Z-DNA probe was used for both bandshift and Southwestern assays.

Mutant and wild-type $\text{Z}\alpha$ proteins were tested for specific binding to Z-DNA by bandshift assays using non-denaturing 6 % polyacrylamide gel electrophoresis [16]. For each lane, $\text{Z}\alpha$ protein was incubated with 100 pg Z-DNA probe (~ 40000 cpm) for 10 min in a 20 μL reaction volume containing 1 μg of sonicated salmon sperm DNA, 10 mM MgCl_2 , 25 mM NaCl and 25 mM Tris/HCl (pH 7.4). After addition of 2 μL loading buffer (Bromphenolblue in a saturated Ficoll solution), the samples were loaded on a 20 cm gel and separated by electrophoresis at 250 V. The bands were visualized by autoradiography using Reflection NEF 496 film (Dupont).

The Southwestern assay combines a Western blot with Z-DNA probe detection (the „Southern“ part of the assay) [17]. Mutant GST-fusion proteins were separated by standard 15 % SDS-polyacrylamide gel electrophoresis and blotted onto a 0.2 μm reinforced nitrocellulose membrane (BioRad) in Tris/glycine buffer (25 mM Tris, 192 mM glycine), 20 % methanol at 4° C using an electric field of 200 V (Mini-Protean II System, BioRad). Colored molecular mass markers (BioRad) were used as standards. The membrane was blocked twice for 30 min each in approximately 15 mL PBS, 0.5 % Igepal (Sigma), 5 mM DTT and 1 % BSA. After washing twice with 15 mL PBS, 0.5 % Igepal for 10 min each, approximately 5 ng Z-DNA probe ($\sim 2 \cdot 10^6$ cpm), 100 μg sonicated salmon sperm DNA and 16 mM MgCl_2 were briefly pre-incubated in a volume of 250 μL , diluted with 5 mL PBS, 0.5 % Igepal and incubated with the membrane for 45 – 90 min. After washing three times with PBS, 0.5 % Igepal, the membrane was dried and exposed to an autoradiography film (Reflection NEF 496, Dupont).

The amount of protein blotted onto the membrane was determined by Western blot. The wet membrane was incubated with 5 μL anti-GST-antibody (Pharmacia) in 5 mL PBS, 0.5 % Igepal for 45 min. After three washing steps with 5 mL PBS, 0.5 % Igepal, the membrane was incubated with 1 μL of the secondary antibody anti-(GST-antibody)-alkalic-phosphatase for 45 min. After washing twice with 10 mL PBS, 0.5 % Igepal, the membrane was incubated with 5 mL alkalic phosphatase substrate mix (BCIP/NBT, Kirkegaard & Perry) until clear intense bands emerged (5 – 10 min).

GST-fusion mutant proteins showed a varying extent of C-terminal proteolytic degradation *in vivo* [5]. By using Z-DNA probe detection and Western blot in conjunction on the same membrane, the proteolytic fragments could be separated by molecular weight and individually tested for binding to Z-DNA. Since only full length protein bound to Z-DNA, the amount of full length protein used for Southwestern assays was adjusted to give Western blot bands of equal intensity.

NMR spectroscopy

NMR experiments were carried out on 1.8 - 2 mM samples in 10 mM Na-phosphate buffer (pH 5), 137 mM NaCl and 0.1 mM NaN₃ (10% D₂O) at 25° C on 500, 600 and 750 MHz NMR spectrometers (self-built instruments at Francis Bitter Magnet Laboratory, MIT, Cambridge) and 600 and 750 MHz NMR spectrometers (Bruker instruments at FMP, Berlin). ¹H, ¹⁵N and ¹³C resonance assignments were obtained from the following 3D heteronuclear correlation NMR experiments [18]: ¹⁵N-HSQC-TOCSY, CBCA(CO)NH, CBCANH, HBHA(CO)NH, H(CCO)NH, HCCH-COSY, HCCH-TOCSY and HNHA.

³J_{HNHA} coupling constants were measured from a 3D HNHA spectrum (ξ=14ms) using integrated diagonal and cross peaks. Apparent coupling constants were multiplied by a factor of 1.11 to correct for H α spin flips [19].

Interproton distance restraints were derived from 3D ¹⁵N-HSQC-NOESY (70, 150 and 250 ms mixing times), 3D ¹³C-HSQC-NOESY (40, 70 and 100 ms mixing times for aliphatic region; 35 and 70 ms mixing times for aromatic region) and 2D NOESY in D₂O and H₂O (20, 40, 80 and 160 ms mixing times). Spectra were processed with NMRpipe [20] or XwinNMR (Bruker GmbH) and analyzed with FELIX'97 (MSI Inc.). 2D strips from 3D ¹⁵N-HSQC-NOESY experiments were extracted and sequentially aligned using the programs Pipp and Plotseq [21]. Spectra were indirectly referenced through the magnetogyric ratios by external calibration on DSS [22].

Interaction mapping

For interaction mapping, 2D ¹⁵N-HSQC spectra were recorded on free Z α and (Z α)₂/Z-DNA complex in the same buffer as described above at 25 °C. The sample of the complex was prepared by titrating Z α into d(CG)₃T₄(CG)₃ DNA at diluted concentrations, and concentrated by ultrafiltration using a stir cell (Amicon, Millipore Corp.). Free d(CG)₃T₄(CG)₃ forms a hairpin with a 6 basepair d(CG)₃ stem in the B-DNA conformation in solution [4]. The saturation level of 2 Z α to 1 hairpin was monitored by 1D ¹H-NMR on well-resolved resonances. Spectra were processed and analyzed as described above.

Structure calculation

NOE restraints derived from all four types of NOESY experiments were analyzed in the conventional manner using a lower boundary of 1.8 Å and an upper boundary of 6 Å and 7 Å for 3D and 2D NOESYs, respectively. Structures were calculated by dynamic simulated annealing from random coordinates [23] at 2000 K using X-PLOR 3.1 [24] and floating stereospecific assignment [25-28]. Intraresidual NOEs were omitted. Force constants for NOE

and phi angle restraints were $50 \text{ kcal mol}^{-1} \text{ \AA}^{-2}$ and $200 \text{ kcal mol}^{-1} \text{ rad}^{-2}$, respectively. Force constants for bond lengths, bond angles and improper angles were $1000 \text{ kcal mol}^{-1} \text{ \AA}^{-2}$, $500 \text{ kcal mol}^{-1} \text{ rad}^{-2}$ and $500 \text{ kcal mol}^{-1} \text{ rad}^{-2}$, respectively.

The atomic coordinates of the 15 lowest energy structures of a total of 200 have been deposited in the Protein Data Bank (PDB) and can be retrieved via the internet at: www.rcsb.org with the PDB ID code: 1qgp.